CrystEngComm

Accepted Manuscript

This article can be cited before page numbers have been issued, to do this please use: A. Lazi, N. Trišovi, L. Radovanovi, J. Rogan, D. Poleti, Ž. Vitnik, V. Vitnik and G. Ušumli, *CrystEngComm*, 2016, DOI: 10.1039/C6CE02210C.

ROYAL SOCIETY OF CHEMISTRY

rsc.li/crystengcomm

View Article Online
DOI: 10.1039/C6CE02210C

Journal Name

ARTICLE

Towards understanding intermolecular interactions in hydantoin derivatives: case of cycloalkane-5-spirohydantoins tethered with a halogenated benzyl moiety

Received 00th January 20xx,
Accepted 00th January 20xx

DOI: 10.1039/x0xx00000x

www.rsc.org/

Anita Lazić,[a] Nemanja Trišović,[a] Lidija Radovanović,[b] Jelena Rogan,[a] Dejan Poleti,[a] Željko Vitnik,[c] Vesna Vitnik[c] and Gordana Ušćumlić[c]

A series of cycloalkane-5-spirohydantoins bearing a halogeno substituted benzyl group (X = Cl and Br) in position 3 has been synthesized and their structures (**1–6**) have been determined by single crystal X-ray diffraction method. These compounds have multiple functional groups, which allow a greater competition and/or cooperation among the different intermolecular interactions in formation of their crystal structures. The molecules are linked together by paired N–H···O hydrogen bonds in $R_2^2(8)$ rings, while the C–H···O interactions lead to their further association into double chains. The contribution of the cycloalkyl ring depends on its conformational flexibility and the multiple C–H donor implications. In the case of compounds **1–4** bearing the cyclopentyl or the cyclohexil ring, halogen bonding (X···O) interactions give rise to a supramolecular pseudo-hexagonal network. In addition, the C–H···X interactions with a higher degree of multifurcation at the halogen acceptor have an important role in formation of the crystal structure. Regarding compounds **5** and **6** with the cycloheptane ring, the X···O interaction is absent and, along with the C–H···X interactions, these compounds realize an alternative crystal structure with emphasis on the X···π interactions. The lattice energies of all these crystal structures, as well as intermolecular pair energies, have been calculated using PIXEL and further partitioned into coulombic, dispersive, polarization and repulsive factors. The crystal structures have also been subjected to Hirshfeld surface analysis which reveals that approximately 75% of the close contacts correspond to relatively weak interactions. The application of both concepts has provided a new insight into relationships between molecular and crystal structure of the hydantoin derivatives.

Introduction

Strategies aimed toward generating new supramolecular structures have been mostly focused on the rational design of the self-assembling building blocks and the control of the interplay between intermolecular interactions. In this regard, hydantoin (imidazolidine-2,4-dione), a heterocycle present in various biologically active compounds, represents an attractive structural component with a rigid core and two amide fragments. Despite the fact that the supramolecular structures of its derivatives are governed by the N–H···O hydrogen bonds, substituents attached to the heterocyclic ring delicately influence the overall molecular arrangement. A detailed analysis of crystal structures of hydantoin derivatives in the Cambridge Structural Database[1] has revealed four main types of hydrogen bond motifs: $R_2^2(8)$–1O–tape, $R_2^2(8)$–2O–tape, $R_3^3(12)$–2O–tape and $R_2^2(8)$–dimer in network.[2] Achiral hydantoin derivatives crystallize with the $R_2^2(8)$–2O–tape motifs through inversion symmetry, while chiral compounds usually crystallize with either $R_2^2(8)$–1O–tape or the $R_3^3(12)$–2O–tape motifs which are generated through screw axis symmetry.[2]

Hydantoin derivatives are important anticonvulsant drugs; they are employed for the treatment of neurological disorders such as epilepsy and trigeminal neuralgia. Phenytoin (5,5-diphenylhydantoin) is the most important among them, considering its therapeutic significance and its relevance pertaining to the research of anticonvulsant mechanisms.[3] Mephenytoin (3-methyl-5-ethyl-5-phenylhydantoin) has a spectrum of activity similar to phenytoin, while this drug may exert serious toxic effects.[4] Due to the low efficacy and pharmacokinetic limitations, etothoin (3-ethyl-5-phenylhydantoin) is mostly used as an adjunctive drug in the treatment of generalized tonic-clonic seizures.[5] In addition to anticonvulsant activity, a variety of other biological activities for hydantoin derivatives has been reported including application as antiarrythmic drugs,[6] bactericides[7] and drugs in cancer therapy.[8]

In the pharmaceutical industry crystal packing studies of biologically active compounds are crucial for bioavailability and processing problems. The significance of crystal packing studies of hydantoin derivatives is further enhanced when one recognizes that certain analogies might be drawn between interactions in the crystal packing and interactions with biological matrices.[9] Anticonvulsant activity of hydantoins is mediated by their interaction and inhibition of the voltage-gated sodium channels in brain. Regarding the molecular mode of action of phenytoin, the tendency of its amide

[a] Faculty of Technology and Metallurgy, University of Belgrade, Karnegijeva 4, 11000 Belgrade, Serbia. E-mail: ntrisovic@tmf.bg.ac.rs.
[b] Innovation Center, Faculty of Technology and Metallurgy, University of Belgrade, Karnegijeva 4, 11000 Belgrade, Serbia.
[c] Department of Chemistry, ICTM, University of Belgrade, Studentski trg 12-16, 11000 Belgrade, Serbia.

†Electronic Supplementary Information (ESI) available: Additional data, Table S1 and Fig. S1–S16. CCDC 1509612–1509617 See DOI: 10.1039/x0xx00000x

View Article Online
DOI: 10.1039/C6CE02210C

groups to form hydrogen bonds is transformed into interactions with the aromatic ring of the amino acid residue Phe-1764 to form an amino-aromatic hydrogen bond in the inner pore of the voltage-gated sodium channel.[10]

The exploration of supramolecular structures of hydantoin derivatives has been associated with the study of hydrogen bonding interactions. On the other hand, the formation of different crystal polymorphs also allows the establishment of weak interactions which, when numerous, affect each other.[11] In this context, a series of cycloalkane-5-spirohydantoins bearing a substituted benzyl group in position 3 of the heterocyclic ring has been synthesized here (Fig. 1) and the evolution of their crystal structures has been analyzed. The conformational flexibility within the investigated series of compounds has been altered by increasing the size of the cycloalkyl ring from cyclopentyl to cycloheptyl. We have introduced a halogen substituent (X = Cl and Br) in the benzyl moiety to explore whether their interactions can promote the formation of different structural motifs. The planarity of this aromatic system may facilitate intermolecular interactions of the halogen atoms which are less sterically hindered than in an aliphatic system.

When present in organic compounds, halogens can be involved in a variety of intermolecular interactions. A systematic statistical analysis of the Cambridge Structural Database has revealed that, in comparison to analogous C–H···O and C–H···N interactions, the short C–H···X interactions are less frequent or just sporadic depending on the halogen atom.[12] Formerly considered controversial, these interactions are now regarded as weak hydrogen bonds, where lower coulombic stabilization is compensated by dispersion.[13] Considering their directionality, the C–H···X interactions are easily distorted from linearity and the bent bonds are entropy favoured.[14] On the other hand, in X···O halogen bonds a Lewis base places a region of charge concentration to a region of positive electrostatic potential on the outer side of a halogen atom (σ-hole).[12,15] Despite the fact that dispersion also plays an important role in this interaction, the directionality of the halogen bond results from the coulombic interaction between the σ-hole of a halogen atom and a Lewis base.[16]

When hydrogen bonding and halogen bonding exist simultaneously, the hydrogen atom in hydrogen bonding and the halogen atom in halogen bonding compete with each other as an electron acceptor.[17] The nature and the number of these interactions make prediction of the crystal structure very difficult. To explain the supramolecular preferences of the investigated compounds, we have put emphasis on features which distinguish the halogen bonding from hydrogen bonding, including higher directionality, size of the interacting atom and the possibility to modify the strength of interactions by changing the halogen substituent. By exploring the molecular geometry of the investigated compounds and quantifying the intermolecular interactions based on the Hirshfeld surfaces analysis[18] and the PIXEL method,[19] the present study will help to gain an insight into the relationship between molecular and crystal structure of hydantoin derivatives.

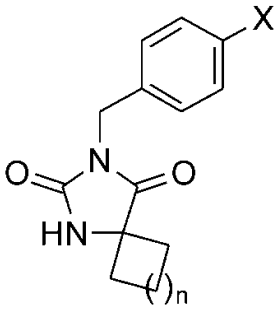

Compound	n	X
1	2	Cl
2	2	Br
3	3	Cl
4	3	Br
5	4	Cl
6	4	Br

Figure 1 Molecular structure of the investigated compounds.

Results and discussion

Molecular structures

Representative ORTEP diagrams of **1**–**6** are shown in Fig. 2. The cyclopentane ring in the compounds **1** and **2** has an envelope conformation, while the cyclohexane ring in the compounds **3** and **4** displays a stable chair conformation (Table S1). The compounds **5** and **6**, on the other hand, crystallize with two molecules in the asymmetric unit (molecules **A** and **B**, Fig. 2), differentiating primarily in the conformation of the cycloheptane ring. This flexible ring adopts a chair conformation in one of the molecules, while it is distorted in the other one with the twisted-chair conformation (Table S1). The N–H bond of the hydantoin ring almost always occupies an axial position[20] and the investigated compounds **1**–**6** are no exception.

Selected molecular geometry parameters of the investigated compounds are presented in Table 1. The bond lengths and angles of the hydantoin moieties are affected by the π-conjugation in the amide fragments,[20] while the size of the cycloalkyl ring has little or no effect on them. The C2=O1 bond is slightly longer than the C4=O2 bond and this difference becomes smaller when the bromo substituent is present in the benzyl moiety. The bonds involving the spirocarbon atom, C4–C5 (average 1.52 Å) and N1–C5 (average 1.46 Å), are the longest in the hydantoin ring as a result of a higher σ character. The other C–N bonds have π character, while the N1–C2 bond (average 1.32 Å) is the shortest among them. The C_{m+5}–C_{m+6} (average 1.51 Å) and N3–C_{m+5} (average 1.45 Å) bonds connecting the hydantoin and phenyl rings show an σ character. It has been demonstrated that the introduction of an electron-withdrawing halogen substituent in the benzyl moiety results in the shortening of the former and the extension of the latter bond when compared to the compound with the unsubstituted benzyl group.[21] Bending of the C2=O1 bond toward N3 is a common structural feature of the hydantoin moiety.[20] The O1–C2–N1 angle is greater than the O1–C2–N3 angle for *ca*. 5°, which results from a stronger repulsion between the lone pairs of the carbonyl oxygen O1 and the electron pairs in the N3–C2 bond. The corresponding angles around C4 are practically the same (Table 1).

As expected, the hydantoin moiety is almost planar in all cases. With the exception of molecules **5B** and **6A**, the planes defined by the hydantoin ring and cycloalkane are nearly perpendicular with the corresponding dihedral mean plane angles ranging from 86.8° in **5A** to 89.9° in **1** (Table 2). The planes of the hydantoin ring and the phenyl ring stand in the similar relationship, while the planes of the phenyl ring and cycloalkane are nearly parallel. These observations are comparable with those commonly observed in cycloalkane-5-spirohydantoins and other structurally related compounds.[20]

View Article Online
DOI: 10.1039/C6CE02210C

Journal Name

ARTICLE

Table 1 Selected bond lengths (Å) and angles (°) in the investigated compounds

	1	2	3	4	5		6	
					A	B	A	B
N1–C2	1.333(3)	1.336(4)	1.334(2)	1.334(5)	1.330(3)	1.336(3)	1.335(4)	1.335(4)
N1–C5	1.455(3)	1.456(3)	1.459(2)	1.469(5)	1.453(3)	1.458(3)	1.464(5)	1.458(4)
O1–C2	1.219(3)	1.217(3)	1.220(2)	1.224(5)	1.224(3)	1.222(3)	1.222(4)	1.218(4)
C2–N3	1.397(3)	1.401(4)	1.401(2)	1.403(5)	1.396(3)	1.392(3)	1.395(4)	1.392(4)
N3–C4	1.372(3)	1.370(4)	1.372(2)	1.375(5)	1.367(3)	1.365(3)	1.366(4)	1.373(4)
O2–C4	1.200(3)	1.210(4)	1.206(2)	1.214(5)	1.207(3)	1.207(3)	1.205(4)	1.203(4)
C4–C5	1.515(3)	1.516(4)	1.511(2)	1.512(5)	1.523(3)	1.523(3)	1.523(4)	1.527(5)
C_{m+5}–C_{m+6}	1.508(3)	1.510(4)	1.509(2)	1.512(5)	1.508(3)	1.507(3)	1.511(4)	1.504(4)
N3–C_{m+5}	1.448(3)	1.455(4)	1.453(2)	1.447(5)	1.450(3)	1.457(3)	1.455(4)	1.448(5)
C2–N1–C5	113.2(2)	113.3(2)	113.1(2)	112.8(3)	113.6(2)	113.2(2)	113.1(3)	113.4(3)
O1–C2–N1	128.9(2)	129.0(3)	128.6(2)	128.4(4)	128.8(2)	128.6(2)	128.4(3)	128.7(3)
O1–C2–N3	123.9(2)	124.0(2)	124.0(2)	123.7(3)	123.8(2)	124.1(2)	123.9(3)	123.7(3)
N1–C2–N3	107.7(2)	107.0(2)	107.4(1)	107.8(3)	107.4(2)	107.4(2)	107.6(2)	107.6(3)
C2–N3–C4	111.5(2)	111.5(2)	110.9(1)	110.5(3)	111.2(2)	111.4(2)	111.2(2)	111.2(2)
O2–C4–N3	125.9(3)	125.3(3)	125.6(2)	125.9(3)	125.5(2)	125.7(2)	125.4(3)	125.8(3)
O2–C4–C5	127.2(2)	127.6(3)	126.9(3)	126.2(4)	127.2(2)	127.1(2)	127.1(3)	127.1(3)
N3–C4–C5	106.8(2)	107.1(2)	107.6(1)	107.9(3)	107.3(2)	107.2(2)	107.5(3)	107.2(3)
N1–C5–C4	101.2(2)	101.0(2)	100.8(1)	100.6(3)	100.5(2)	100.5(2)	100.4(2)	100.4(2)
C_{m+6}–C_{m+5}–N3	113.7(2)	113.0(2)	115.5(2)	115.4(3)	115.2(2)	113.1(2)	112.9(3)	115.1(3)

m - number of carbon atoms in the cycloalkyl ring

Crystal packing and intermolecular interactions

Compounds **1**–**4** crystallize in the monoclinic space group $P2_1/n$ with $Z = 4$. Interaction energies (I.E.s) of the molecular segments extracted from their crystal structures are presented in Table 3. The distance criterion used for the intermolecular interactions is the sum of the van der Waals radii + 0.4 Å and the directionality is greater than 110°.[22] Regarding that all four compounds have similar structural features, geometries of segments of **2** as a representative compound are shown in Fig. 3. In all cases, the molecules are centrosymmetrically paired through N–H···O hydrogen bonds (Table 4) to form an $R_2^2(8)$ ring (segment I) with I.E. being about –74 kJ mol^{-1}, wherein the coulombic contribution is more significant than the polarization and dispersion contributions. The formation of these characteristic dimers in **3** and **4** is supported by additional bifurcated C–H···O interactions. The dimers then assemble into double chains. Each chain is formed by C–H···O interactions between the carbonyl O1 atom and the hydrogen atoms of the cycloalkyl and phenyl rings (segment II with I.E. of about –34 kJ mol^{-1} which is mainly dominated by the dispersion contribution). The large number of potential donor groups leads to the multifurcated acceptor role of the carbonyl O1 atom. The H···O distance varies between 2.5 and 3.1 Å, while the "softer" directionality of these interactions[23] is reflected in a distortion from the linearity with the average C–H···O angle of 130°. The molecules of opposite chains in the successive dimers are joined together by paired C–H···N interactions in a centrosymmetric $R_2^2(8)$ pseudo-ring (segment III, I.E. = *ca*. –30 kJ mol^{-1} wherein dispersion plays a large role in the stabilization). These interactions are usually regarded as weak hydrogen bonds with structure directing capabilities.[24] Generally, the hydantoin moieties forming a dimer are separated by *ca*. 5.5 Å, while the distance between the successive rings is *ca*. 6.0 Å.

The supramolecular complexity of the investigated compounds arises from the cross-linking of the neighbouring dimers through interactions involving halogens (X···O and C–H···X;) which generate a supramolecular pseudo-hexagonal network (Fig. 4a). While exploring the role of substituents on the cyclohexyl ring in the

Table 2 Dihedral angle (°) between the mean planes defined by the ring units in the investigated compounds

Compound		cycAlk–Hyd	Hyd–Ph	cycAlk–Ph
1		89.9(1)	88.4(1)	9.45(1)
2		89.8(1)	88.8(1)	14.4(1)
3		88.9(1)	77.4(1)	12.0(1)
4		88.1(1)	80.4(1)	11.8(1)
5	**A**	86.8(1)	81.8(1)	13.8(1)
	B	75.3(1)	76.3(1)	6.23(1)
6	**A**	75.4(1)	76.4(1)	5.48(1)
	B	87.3(1)	81.3(1)	13.0(1)

Hyd-plane of the hydantoin ring; cycAlk- plane of the cycloalkyl ring; Ph-plane of the phenyl ring.

View Article Online
DOI: 10.1039/C6CE02210C

crystal structure of cyclohexenespiro-5-hydantoin derivatives, Graus *et al.* have observed the formation of a 2D network in 4-carboxylic-cyclohexanespiro-5-hydantoin acid, which also consists of $R_6^6(46)$ rings.[9c] In this case, supramolecular rectangles are built of four coplanar $R_2^2(8)$ rings linking the hydantoin moieties and two perpendicular $R_2^2(8)$ rings formed by the carboxylic groups. This situation opens up the possibility for the formation of a porous structure. To analyze and compare the corresponding I.E.s, reductions in the halogen bond length relative to the sum of the atomic radii for halogens and oxygen should be taken into account. In the case of the Br···O interaction, the larger reduction results in a larger coulombic contribution, but also repulsion contribution due to the molecular overlap. The effect of replacing the chloro substituent with the bromo substituent on decomposition of I.E. is somehow more expressed in cyclopentane-5-spirohydantoins than in cyclohexane-5-spirohydantoins. A significant dispersion contribution is needed to achieve the overall stabilization. In segment VI of compounds **1**–**4** where two C–H···X interactions are also operative, the dispersion contribution exceeds the total energy, thus being a net overcompensation for repulsion.

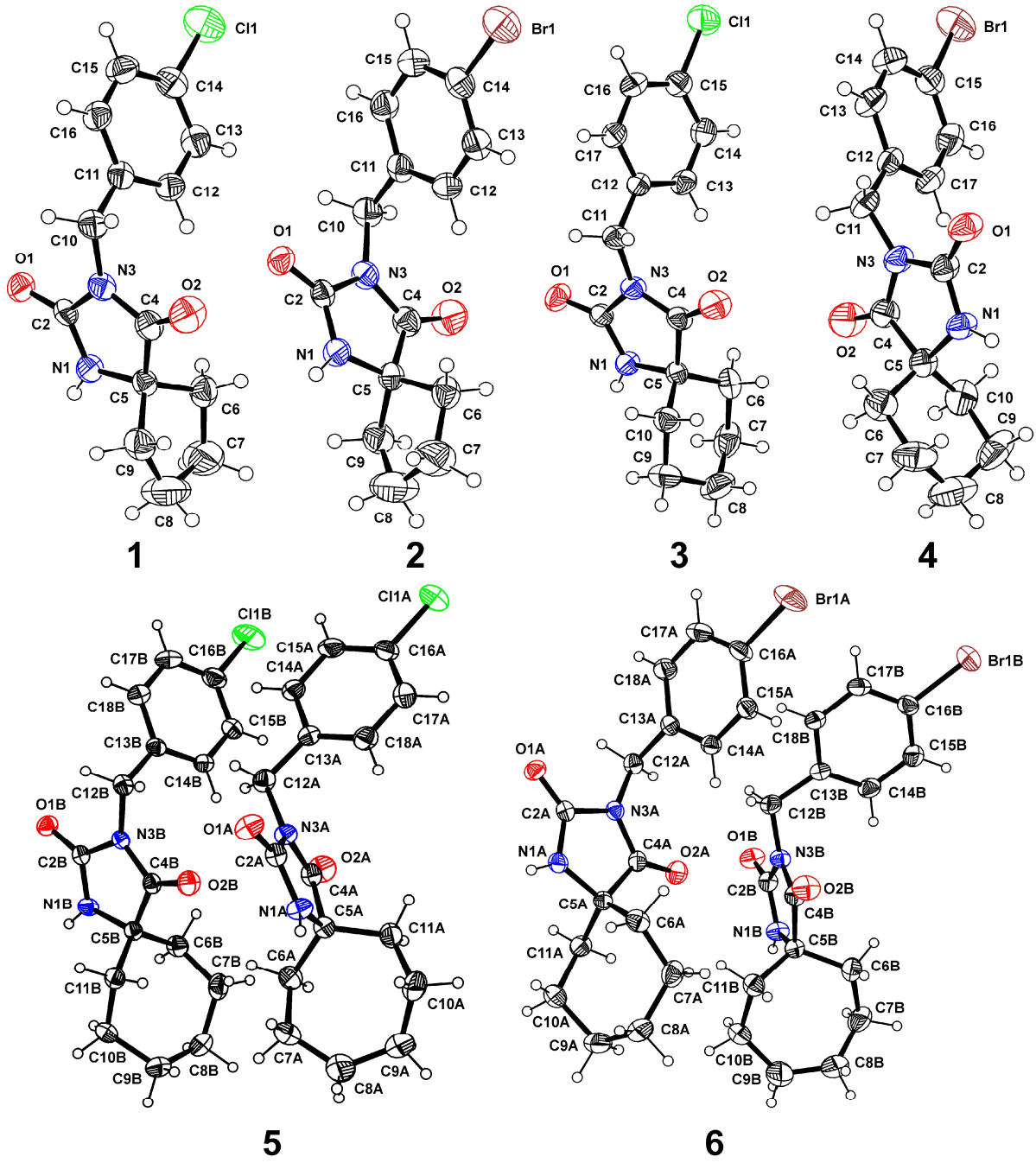

Figure 2 Molecular structures of the investigated compounds with the atomic numbering schemes (Displacement ellipsoids are drawn at the 50% probability level for compounds **1**–**4** and at the 30% probability level for compounds **5** and **6**); the H atoms are shown as small spheres of arbitrary radii.

View Article Online
DOI: 10.1039/C6CE02210C

Table 3 PIXEL interaction energies (I.E.; kJ mol^{-1}) in the extracted molecular segments related by a symmetry operation and the corresponding intermolecular interactions

	Distance[a], Å	E_{coul}	E_{pol}	E_{disp}	E_{rep}	E_{tot}	Symmetry	Important interactions
Compound 1								
I	7.567	–89.9	–34.9	–26.5	75.9	–75.5	$-x+1, -y+1, -z+1$	N1–H1···O1
II	5.875	–10.2	–5.8	–36.1	18.6	–33.5	$x, y-1, z$	C6–H6A···O1, C12–H12···O1, C13–H13···O1
III	6.305	–3.7	–5.8	–39.3	19.9	–28.9	$-x+1, -y+1, -z+1$	C6–H6A···N1
IV	6.581	–6.9	–4.5	–28.4	17.5	–22.3	$-x+1/2, y+1/2, -z+3/2$	C15–H15···O2, C16–H16···O2, C10–H10B···π
V	9.997	–6.0	–1.3	–13.4	6.0	–14.7	$x-1/2, -y+1/2, z-1/2$	C9–H9B···Cl1
VI	10.815	–4.3	–2.4	–14.0	8.6	–12.1	$x-1/2, -y-1/2, z-1/2$	C6–H6B···Cl1, C9–H9A···Cl1, Cl1···O2
VII	12.667	–6.0	–3.0	–13.6	10.4	–12.1	$-x+1, -y, -z+2$	C15–H15···Cl1
Compound 2								
I	8.484	–85.5	–30.9	–26.2	72.3	–70.3	$-x+1, -y, -z+1$	N1–H1···O1
II	5.926	–9.8	–5.5	–35.6	18.1	–32.8	$x, y+1, z$	C6–H6B···O1, C12–H12···O1, C13–H13···O1
III	6.906	–5.2	–6.3	–40.9	21.7	–30.5	$-x+1, -y+1, -z+1$	C6–H6B···N1
IV	6.251	–5.4	–4.1	–27.3	15.7	–21.1	$-x+1/2, y-1/2, -z+3/2$	C16–H16···O2, C10–H10B···π
V	10.174	–5.6	–1.0	–12.2	4.7	–14.2	$x-1/2, -y+1/2, z-1/2$	C9-H9A···Br1
VI	10.693	–8.0	–2.8	–14.2	12.4	–12.5	$x-1/2, -y+3/2, z-1/2$	C6–H6A···Br1, C9–H9B···Br1, Br1···O2
VII	11.358	–5.8	–2.3	–13.7	11.3	–10.4	$-x+1, -y+1, -z+2$	C15–H15···Br1
Compound 3								
I	7.779	–81.1	–29.0	–28.5	65.3	–73.3	$-x+1, -y+1, -z+1$	N1–H1···O1, C7-H7A···O1, C7–H7B···O1
II	5.913	–9.7	–5.5	–36.2	17.1	– 34.4	$x, y-1, z$	C13–H13···O1, C6–H6B···O1
III	6.350	–5.8	–5.3	–39.2	19.6	–30.7	$-x+1, -y, -z+1$	C6–H6B···N1, C7–H7B···O1
IV	6.689	–10.1	–6.0	–30.7	22.9	–23.8	$-x+1/2, y+1/2, -z+3/2$	C11–H11···π, C17–H17···O2, C16–H16···O2

[a]Distance between centers of mass.

View Article Online
DOI: 10.1039/C6CE02210C

Table 3 *(Continued)*

	Distance[a], Å	E_{coul}	E_{pol}	E_{disp}	E_{rep}	E_{tot}	Symmetry	Important interactions
Compound 3								
V	10.653	–5.9	–1.6	–15.7	8.1	–15.1	$x - 1/2, -y + 1/2, z - 1/2$	C10–H10B···Cl1
VI	11.325	–4.7	–2.8	–15.7	9.6	–13.5	$x - 1/2, -y - 1/2, z - 1/2$	C6–H6A···Cl1, C10–H10A···Cl1, Cl1···O2
VII	13.745	–3.8	–1.7	–10.4	5.4	–10.4	$-x + 1, -y, -z + 2$	C16–H16···Cl1
Compound 4								
I	8.843	–82.5	–30.1	–28.3	64.3	–76.6	$-x + 1, -y, -z + 1$	N1–H1···O1, C7–H7B···O1, C9–H9B···O1
II	5.934	–9.8	–5.1	–35.6	16.8	–33.7	$x, y + 1, z$	C17–H17···O1
III	7.126	–5.7	–4.9	–39.2	19.7	–30.2	$-x + 1, -y + 1, -z + 1$	C10–H10A···N1, C9–H9A···O1
IV	6.104	–9.3	–5.5	–30.3	21.7	–23.4	$-x + 3/2, y - 1/2, -z + 1/2$	C11–H11B···π, C13–H13···O2, C14–H14···O2
V	10.997	–5.2	–1.2	–13.3	6.5	–13.2	$x + 1/2, -y + 1/2, z + 1/2$	C6–H6A···Br1
VI	11.346	–5.8	–2.4	–14.4	10.2	–12.3	$x + 1/2, -y + 3/2, z + 1/2$	C6–H6B···Br1, C10–H10B···Br1, Br1···O2
VII	12.414	–3.4	–1.4	–10.3	6.4	–8.7	$-x + 1, -y + 1, -z$	C14–H14···Br1
Compound 5 (A···A)								
I	7.902	–90.1	–34.3	–30.7	75.4	–79.9	$-x, -y + 1, -z + 1$	N1A–H1A···O1A C7A–H7A1···O1A, C10A–H10B···O1
II	6.757	–5.6	–4.5	–35.9	15.6	–30.5	$-x - 1, -y + 1, -z + 1$	C10A–H10A···O1A
III	6.434	–4.6	–3.1	–26.5	8.9	–25.3	$x - 1, y, z$	C11A–H11B···O1
IV	9.781	–1.7	–1.2	–22.3	7.1	–14.7	$-x - 1, -y + 2, -z + 1$	Cl1A···π
V	13.594	–4.0	–2.7	–14.8	12.3	–9.4	$x, y - 1, z$	C9–H9A2···Cl1A
VI	12.026	–2.1	–1.7	–11.6	6.1	–9.3	$-x - 2, -y + 2, -z + 1$	C17A–H17A···Cl1A
A···B/B···A								
VII	5.488	–12.3	–7.2	–42.4	28.1	–33.8	$x - 1, y, z$	C11B–H11D···O2A, lp(O2A) ···π
VIII	5.616	–12.4	–6.9	–42.0	27.7	–33.5	x, y, z	C12–H12B···O2B, C6A–H6A1···O2B lp(O2B) ···π
IX	13.438	–2.5	–1.5	–11.9	6.3	–9.5	$x, y - 1, z$	C8A–H8A2···Cl2B
B···B								
X	7.574	–77.0	–24.8	–22.0	60.8	–63.0	$-x + 1, -y + 1, -z + 2$	N1B–H1B···O1B
XI	4.707	–15.7	–8.5	–69.6	37.4	–56.4	$-x, -y + 1, -z + 2$	C7B–H7B2···O1B, C6B–H6B2···N1B, C8–H8B1···π
XII	6.434	–12.7	–7.3	–37.3	25.7	–31.6	$x - 1, y, z$	C15B–H15B···O1B, C14B–H14B···O1B, C7B–H7B2···N1B

[a]Distance between centers of mass.

View Article Online
DOI: 10.1039/C6CE02210C

Table 3 *(Continued)*

	Distance[a], Å	E_{coul}	E_{pol}	E_{disp}	E_{rep}	E_{tot}	Symmetry	Important interactions
Compound 6 (A···A)								
I	8.455	–81.4	–27.8	–22.2	63.2	–68.3	$-x+1, -y, -z$	N1A–H1A1···O1A
II	5.221	–16.2	–8.9	–71.2	39.1	–57.2	$-x+2, -y, -z$	C7A–H2A···O1A, C6A–H1A···N1A, C8A–H3B···π
III	6.458	–13.2	–7.3	–37.3	25.3	–32.5	$x+1, y, z$	C14A–H12···O1A, C15A–H13···O1A, C7A–H2A···N1A
A···B/B···A								
IV	5.670	–13.4	–7.1	–43.5	29.0	–34.9	x, y, z	C18B–H32···π, C12B– H26A···O2A, C11B–H22B···O2A, lp(O2A) ···π
V	5.576	–12.6	–7.0	–42.8	28.7	–33.7	$x-1, y, z$	C11A–H6A···O2B, lp(O2B) ···π
VI	13.612	–3.1	–1.3	–12.2	5.9	–10.7	$x, y-1, z$	C9B – H20A···Br1A
B···B								
VII	9.145	–85.8	–33.5	–30.8	73.6	–76.4	$-x+2, -y, -z+1$	N1B–H1B1···O1B, C7B–H18A···O1B, C10B–H21B···O2B
VIII	7.640	–5.2	–4.1	–35.3	14.6	–30.1	$-x+3, -y, -z+1$	C7B–H18B···O1B
IX	6.458	–4.2	–3.0	–27.2	9.6	–24.7	$x+1, y, z$	C6B–H17A···O1B
X	8.484	–0.4	–1.3	–22.9	8.8	–15.0	$-x+3, -y-1, -z+1$	Br1B···π
XI	13.713	–4.2	–2.4	–16.2	11.9	–11.0	$x, y+1, z$	C8B–H19A···Br1B

[a]Distance between centers of mass.

Table 4 Hydrogen bonding geometry (Å, °)

Compound	D–H···A	*d*(D–H)	*d*(D···A)	*d*(H···A)	D–H···A
1	N1–H1···O1^{i}	0.86	2.874(3)	2.02	173
2	N1–H1···O1^{ii}	0.86	2.883(3)	2.03	172
3	N1–H1···O1^{i}	0.86	2.927(2)	2.07	173
4	N1–H1···O1^{ii}	0.86	2.930(4)	2.07	174
5	N1A–H1A···O1A^{iii}	0.86	2.886(3)	2.03	171
	N1B–H1B···O1B^{iv}	0.86	2.892(3)	2.06	163
6	N1A–H1A1···O1A^{v}	0.86	2.892(3)	2.06	163
	N1B–H1B1···O1B^{vi}	0.86	2.894(4)	2.04	170

Symmetry codes: (*i*): $-x+1, -y+1, -z+1$; (*ii*): $-x+1, -y, -z+1$; (*iii*): $-x, -y+1, -z+1$, (*iv*): $-x+1, -y+1, -z+2$; (*v*): $-x+1, -y, -z$, (*vi*): $-x+2, -y, -z+1$.

Regarding the geometry of the X···O halogen bonds in segment VI (Table 5), there is a strong preference for a closely linear approach of the carbonyl O2 acceptor toward the halogen as indicated by the D–X···A angle of *ca*. 170°. The angle of approach of the halogen to the carbonyl O2 atom of *ca*. 120° reflects that, according to the σ-hole model,[15] the σ-hole of the halogen is attracted to the non-bonding orbitals of the carbonyl oxygen atom. These values are in accordance with those observed in small molecule structures.[25] The differences in geometric parameters of the halogen bonding in the cyclopentane-5-spirohydantoins (**1**, **2**) and cyclohexane-5-spirohydantoins (**3**, **4**) may be attributable to the steric interactions between the halogen and the cycloalkyl ring (Table 5). Furthermore, the halogen bond shares the carbonyl O2 atom with the C–H···O interaction (segment IV) as the common acceptor, while the directions of these interactions are nearly orthogonal to each other. This can be explained by the fact that the non-bonding orbitals of the carbonyl O2 atom are occupied by this weak hydrogen bond and the only electronegative potential available for the halogen bonding comes from the carbonyl π orbitals.[26] In addition to the C–H···O interactions, segment IV (I.E. ~ –22.6 kJ mol^{-1}) shows that an

Table 5 Geometric Parameters for Halogen Bonds (Å, °)

Compound	*d*(C–X···O)	C–X···O	X···O–C
1	3.284	174.7	122.6
2	3.220	173.8	124.9
3	3.673	165.0	115.9
4	3.684	165.0	117.6

View Article Online
DOI: 10.1039/C6CE02210C

interplay of the benzyl groups offers the potential for the C–H···π interactions. The formation of the network is supported by the C–H···X interactions characterized by distances in the range from 2.9 to 3.1 Å and a slight deviation from linearity (138° < C–H···X angle < 158°) (segments V and VI). Another molecular pair forms an $R_2^2(8)$ pseudo-ring formed via head-to-head C–H···X interactions with H···X distances of 3.0 Å and C–H···X angle of 154.5°, which in the case of compounds **1** and **2** is not planar, but has approximately chair conformation (segment VII, I.E. ~ –10.5 kJ mol^{-1}). In this way, zigzag chains are generated from altering $R_2^2(8)$ rings formed by two types of intermolecular interactions, *i.e.*, N–H···O and C–H···X bonds (Fig. 4b). When comparing the chloro derivatives and the bromo derivatives, replacement of the halogen substituent generally affects only the geometry of the C–H···X bonds. The C–H···Br bonds are slightly longer.

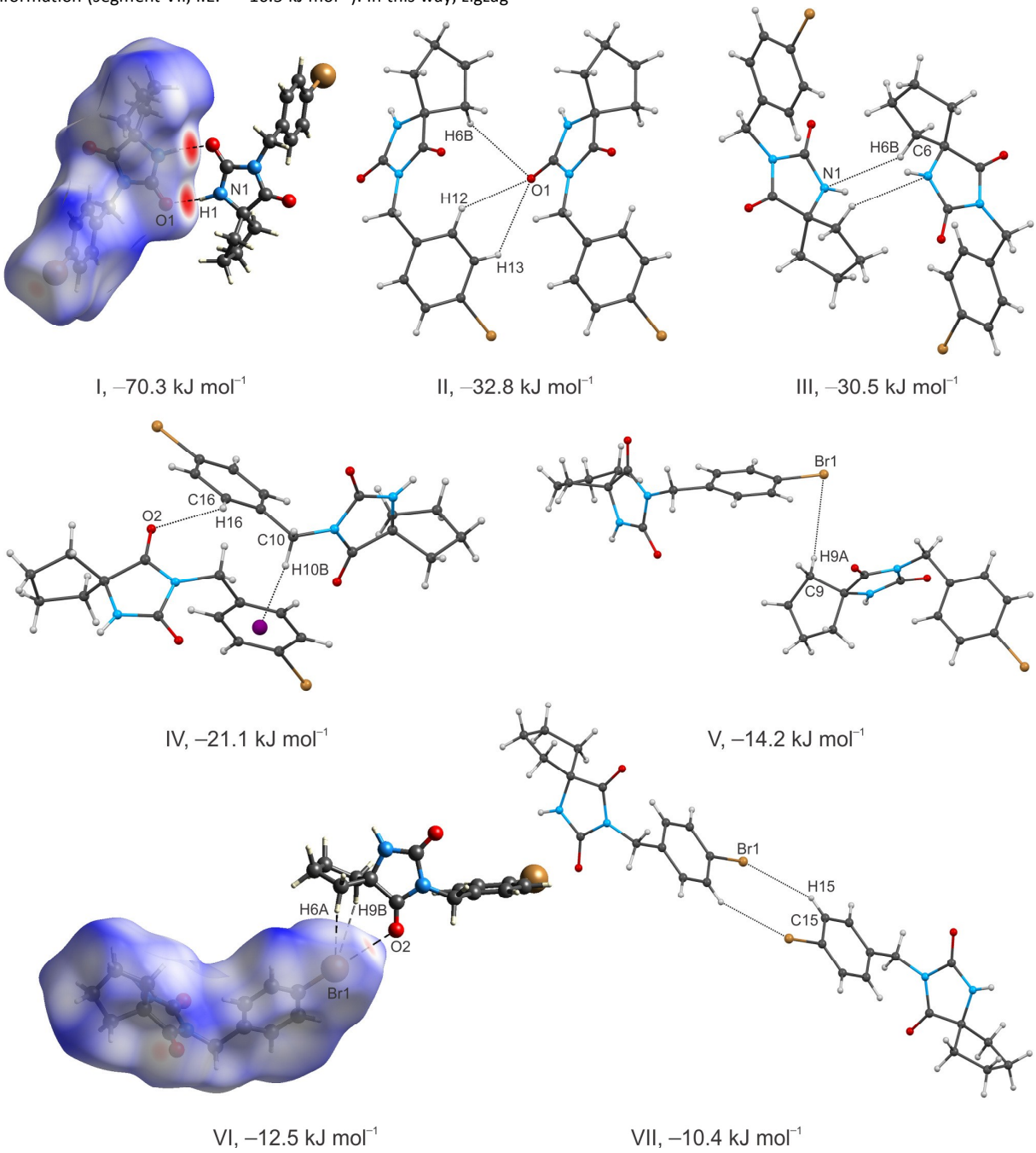

Figure 3 Molecular segments of **2** with decreasing interaction energy (Table 3), showing the most important intermolecular interactions. Hirshfeld surface mapped with d_{norm} is presented in segments I and VI.

View Article Online
DOI: 10.1039/C6CE02210C

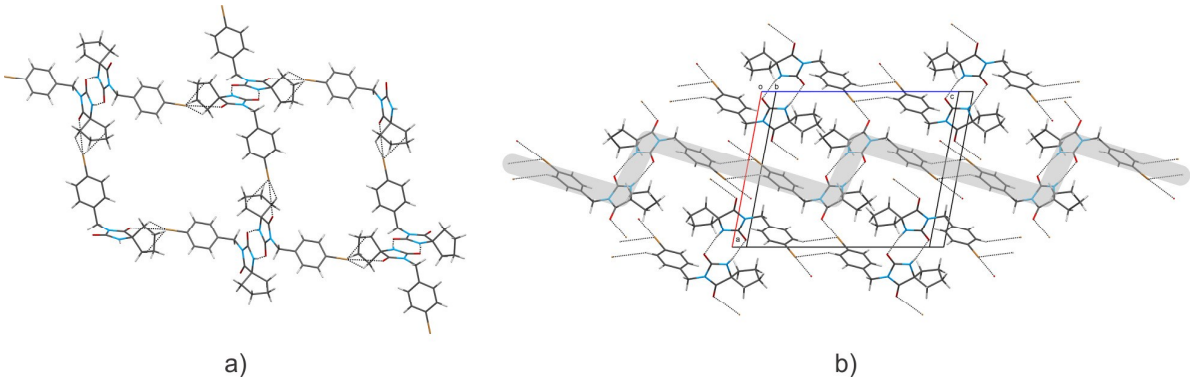

Figure 4 a) Part of the crystal structure of **2**, showing the linking of the hydrogen-bonded $R_2^2(8)$ dimers by C–H···Br and O···Br interactions to generate a supramolecular pseudo-hexagonal network; b) Part of the crystal structure of **2**, showing the formation of a zigzag chain of $R_2^2(8)$ rings through N–H···O and C–H···Br hydrogen bonds (projection approximately onto the *ac*–plane).

Compounds **5** and **6** crystallize with two molecules in the asymmetric unit in the $P\bar{1}$ space group with Z = 4. A variety of modes of association can be identified in these crystals and we have put emphasis on the intermolecular interactions with I.E. ≥ 10 kJ mol^{-1} (Table 3). Because their structural features are closely related to each other, only geometries of segments extracted from the crystal structure of **6** are presented in Fig. 5. Regarding the modes of association, the analogy can be drawn between molecules **5A** and **6B**, as well as **5B** and **6A**. The molecules are linked by N–H···O hydrogen bonds forming two $R_2^2(8)$ homodimers (segments I and VII) with I.E.s of –68.3 and –76.4 kJ mol^{-1} for molecules **6A** and **6B**, respectively; the main contribution to these interactions is a coulombic stabilization. Relative to molecule **6A**, the increase in I.E. for molecule **6B** comes from the contribution of additional C–H···O interactions (segment VII), thus reflecting their difference in the conformation of the cycloheptyl ring.

Characteristic structural features of compounds **5** and **6** result from the formation of two double chains made of the $R_2^2(8)$ rings along *a*-axis where the principal mode of intermolecular aggregation involves the C–H···O hydrogen bonds between molecules of the same chain including both cycloheptyl and benzyl moieties as weak donors and the carbonyl O1 atom as an acceptor (segments II, III, VIII and IX). Analogously to compounds **1**–**4**, the C–H···N interactions further stabilizes this arrangement of molecules A (segments II and III). Along with these interactions, segment II shows that dimers of the molecules **6A** are linked by paired C–H···π interactions involving the π system of the benzyl group.

Alternatively, the crystal packing of these compounds may be regarded as two double chains (Fig. 6) which are formed from the above mentioned hydrogen-bonded $R_2^2(8)$ homodimers linked through a C–H···X interaction (segment XI with I.E. less than –10.0 kJ mol^{-1}). The geometry of these interactions is characterized by a H···X distance of *ca*. 3.1 Å and C–H···X angle of 145°. In the case of the molecule **6B**, the dimerization of the chains is supported by the head-to-head C–Br···π interaction with I.E. of –15 kJ mol^{-1} where the dispersion contribution is the most important (segment X). This interaction is characterized by the Br···centroid distance of 3.943 Å and the distance between both phenyl ring centroids of 4.535 Å, which is consistent with the values seen in small molecule structures for the offset parallel stacking orientation with the phenyl ring planes parallel to each other.[27] The same dimeric segment can also be recognized for the molecule **5A**. In this case, the shorter C–X···π distance results in an increase of the coulombic contribution and a slight decrease of repulsion. However, irrespective of the length of the interaction, the dispersion plays the major role here. The neighboring double chains consisting of different conformers are then cross-linked into a three-dimensional framework by the principal action of C–H···O and lp(O)···π interactions involving the hydantoin π system (segments IV and V with the average I.E. of 34 kJ mol^{-1}). Regarding the latter interactions, the carbonyl group of one hydantoin ring takes a more or less head-on approach toward the centroid of another hydantoin ring with O···centroid distances between 3.2 and 3.5 Å. Segment IV shows adjacent molecules **6A** and **6B** which adopt an edge-to-face geometry with a 51.1(1)° dihedral angle between the phenyl rings. Along with the C–H···O interactions, this arrangement enables the C–H···π interactions. A C–H···X interaction with a H···X distance of 3.152 Å and C–H···X angle 160° is also cooperative in this sense (segment VI, I.E. –10 kJ mol^{-1}). In the case of molecule **6B**, the neighboring double chains are interconnected through pairs of very weak C–H···X interactions (I.E.< 10 kJ mol^{-1}); these connections thus form the centrosymmetric rings of $R_2^2(8)$ type. On the other side, their energetic contribution is more significant in the case of the molecule **5A** (segment VI in Table 3, Fig. S3). Unlike compounds **1**–**4**, no X···O halogen bonding has been identified in the crystal packing of **5** and **6**.

Table 6 lists the total lattice energy of the individual compounds in the range from −142 to −154 kJ mol^{-1} where dispersion, rather than coulombic and polarization, has the major contribution to the total lattice energy.

The described structural features of the investigated compounds are effectively summarized in the Hirshfeld fingerprint plots (Figs 7 and S3), which provide a single map of all the intermolecular atom–atom interactions.[18] It can be observed that the patterns of interactions in the investigated compounds are broadly similar. The H···H interactions occupy nearly 50% of the surface area (Fig. 8). Their contribution increases with the increasing size of the cycloalkyl ring, pointing, among other, to the enhanced dispersion terms in the total lattice energies (Table 6). The shortest H···H

Table 6 Lattice energies partitioned into coulombic, polarization, dispersion and repulsion contribution using PIXEL (kJ mol^{-1})

Compound	E_{coul}	E_{pol}	E_{disp}	E_{rep}	E_{tot}
1	–76.8	–33.0	–146.5	109.6	–146.6
2	–76.4	–30.5	–144.8	109.6	–142.1
3	–76.9	–31.0	–153.9	110.0	–151.9
4	–77.1	–29.4	–149.1	107.7	–147.9
5	–74.9	–31.1	–155.2	110.7	–150.6
6	–77.5	–31.4	–159.0	114.3	–153.7

View Article Online
DOI: 10.1039/C6CE02210C

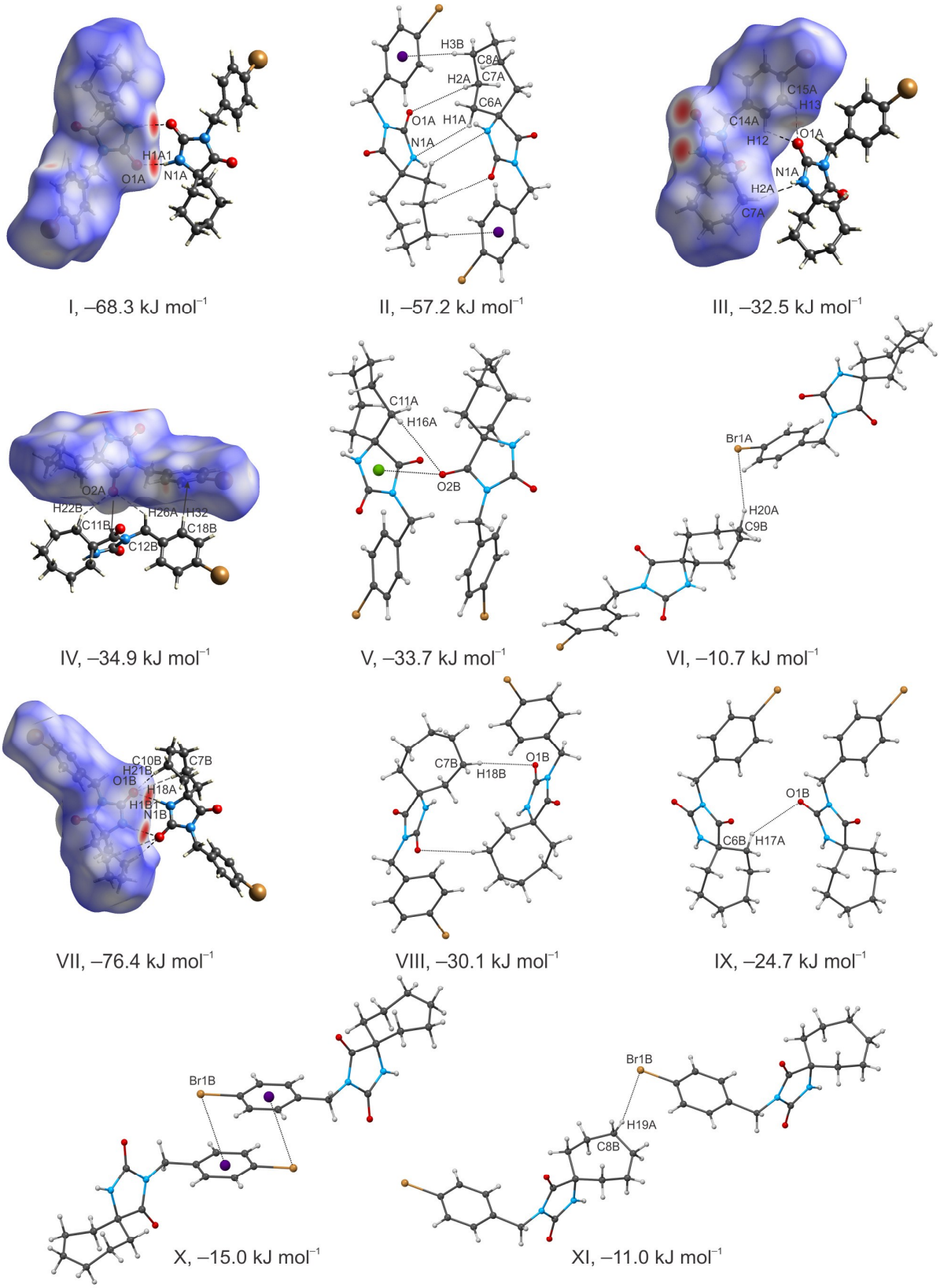

Figure 5 Molecular segments of **6** with decreasing interaction energy (Table 3), showing the most important intermolecular interactions. Hirshfeld surface mapped with d_{norm} is presented in segments I, III, IV and VII.

View Article Online
DOI: 10.1039/C6CE02210C

Journal Name

ARTICLE

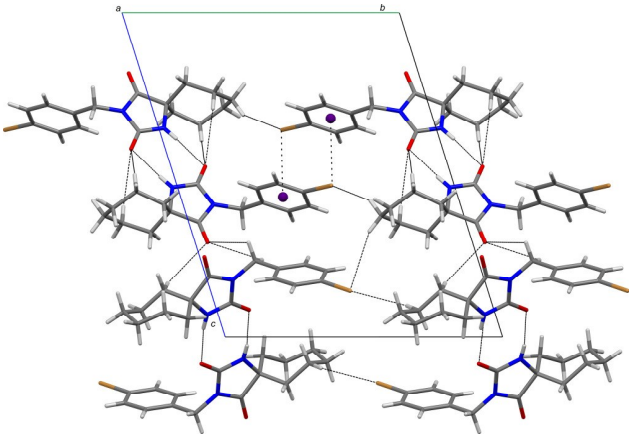

Figure 6 Part of the crystal structure of **6**, showing the linking of the hydrogen-bonded $R_2^2(8)$ homodimers by the C–H···Br and C–Br···π interactions to form double chains (projection onto the *bc*–plane). For clarity, the cross-linking between the neighboring chains by the C–H···Br and C–H···O interactions is only presented.

interactions are presented as broad spikes at $d_e + d_i \approx 2.2–2.4$ Å where a subtle splitting is observed. It is accepted that this splitting is characteristic for a contact between three atoms, rather than for a direct contact between two atoms.[18] A second principal interaction, which accounts from 16 to 20% of the total number of contacts, results from H···O hydrogen bonds. The N–H···O interactions appear as a pair of symmetric spikes extending towards the bottom left ($d_e + d_i \approx 1.8$ Å; the upper spike corresponds to the donor spike, the lower one is the acceptor spike[18]). The investigated crystal structures are further dominated by H···C contacts (associated with C–H···π interactions), which account from 9.5 to 17.5%. This interaction is represented by a pair of wide, well separated wings at $d_e + d_i \approx 2.8–2.9$ Å.

A characteristic hint towards the H···X hydrogen bonds is a pair of broad spikes at longer d_i and d_e (*i.e.*, $d_e + d_i \approx 2.9$ Å) with a greater separation across the diagonal of the plot.[18a] These interactions comprise from 13 to 18% of the surface area. Due to the larger van der Waals radius of the bromine atom, the relative contribution increases slightly in the bromo derivatives when compared to the chloro derivatives with the same cycloalkyl ring. It is also possible to identify other regions of relatively large spot intensity which correspond to intermolecular interactions involving halogens. Around 3% of the whole surface is associated with the X···O bonding in the case of compounds **1–4**, while there is a negligible amount in compounds **5** and **6** (up to 0.5%). The fingerprint for these interactions resembles the hydrogen bonding patterns.[28] It is presented as a pair of two sharp spikes at longer d_i and d_e (*i.e.*, $d_e + d_i \approx 3.2–3.6$ Å) which are somehow longest in compound **2**. Analogously to hydrogen bonding,[29] the stronger halogen bond means more elongated the X···O spike. Regarding molecules **5A** and **6B**, 3% of the whole surface can be identified as X···C contacts which are referred to as C–X···π interactions. This feature appears in the diagonal line of the plot at $d_e = d_i \approx 3.8$ Å. The crystal structures of all the compounds are also described by X···X contacts, but they comprise a negligible proportion of the whole surface area. A detailed inspection of the other intermolecular atom–atom contacts has also revealed a negligible contribution of H···N and C···O (up to 1%).

Figs 3 and 5 contain Hirshfeld surfaces for the molecules in compounds **2** and **6**, which have been mapped over a d_{norm} range from –0.5 to 1.5 Å. This function emphasizes contact distances relative to the sum of van der Waals radii, where the closest contacts are shown in red (negative values of d_{norm}).[18] A pair of equally large red spots corresponds to both donor and acceptor of N–H···O hydrogen bonds. This is characteristic for the $R_2^2(8)$ rings.[30] Additional faint red spots on the Hirshfeld surface of **2** arise from the interactions involving halogens (segment VI, Fig. 3). In the case of compound **6**, the longer H···O contacts, which are associated with C–H···O interactions between the carbonyl O2 atom and the hydrogen atoms of the cycloalkyl and benzyl moieties, show up as two smaller red spots on the Hirshfeld surface (segment IV, Fig. 5). The still longer H···O contacts in segment III are characterised by slightly smaller red spots. Regarding the contacts involving halogens, the final faint red spot indicates a short C–H···Br contact. It has been proven that the analysis of the d_{norm} parameter does not give evidence of the C–X···π interactions,[29] which have been identified in the crystal packing of this compound. Generally, the observations based on the Hirshfeld surface analysis are in a good agreement with the results of the PIXEL analysis.

Conclusions

In this work, a variety of spirohydantoin derivatives has been prepared by the incorporation of a cycloalkyl ring and a substituted benzyl group into the hydantoin ring. This has provided an opportunity to understand the competition and/or the cooperation of the intermolecular interactions, especially those involving halogens, in formation of their crystal structures. Although N–H···O hydrogen bonds dominate, weak interactions lead either to stabilization of the crystal structure (regarding the chloro derivatives relative to the bromo derivatives with the same cycloalkyl ring) or to its alteration (regarding compounds **5** and **6** relative to compounds **1–4**). It has been recognized that the conformational changes of the cycloheptane ring are also stabilized by C–H···O interactions. The PIXEL model has enabled to assess the predominance of interaction modes in the investigated crystal structures. Their ranking in descending order is as follows: molecular pairs containing N–H···O (–63 to –77 kJ mol^{-1}) > molecular pairs containing C–H···N (~ 30 kJ mol^{-1}) > molecular pairs containing C–H···O (–22 to –34 kJ mol^{-1}) >

View Article Online
DOI: 10.1039/C6CE02210C

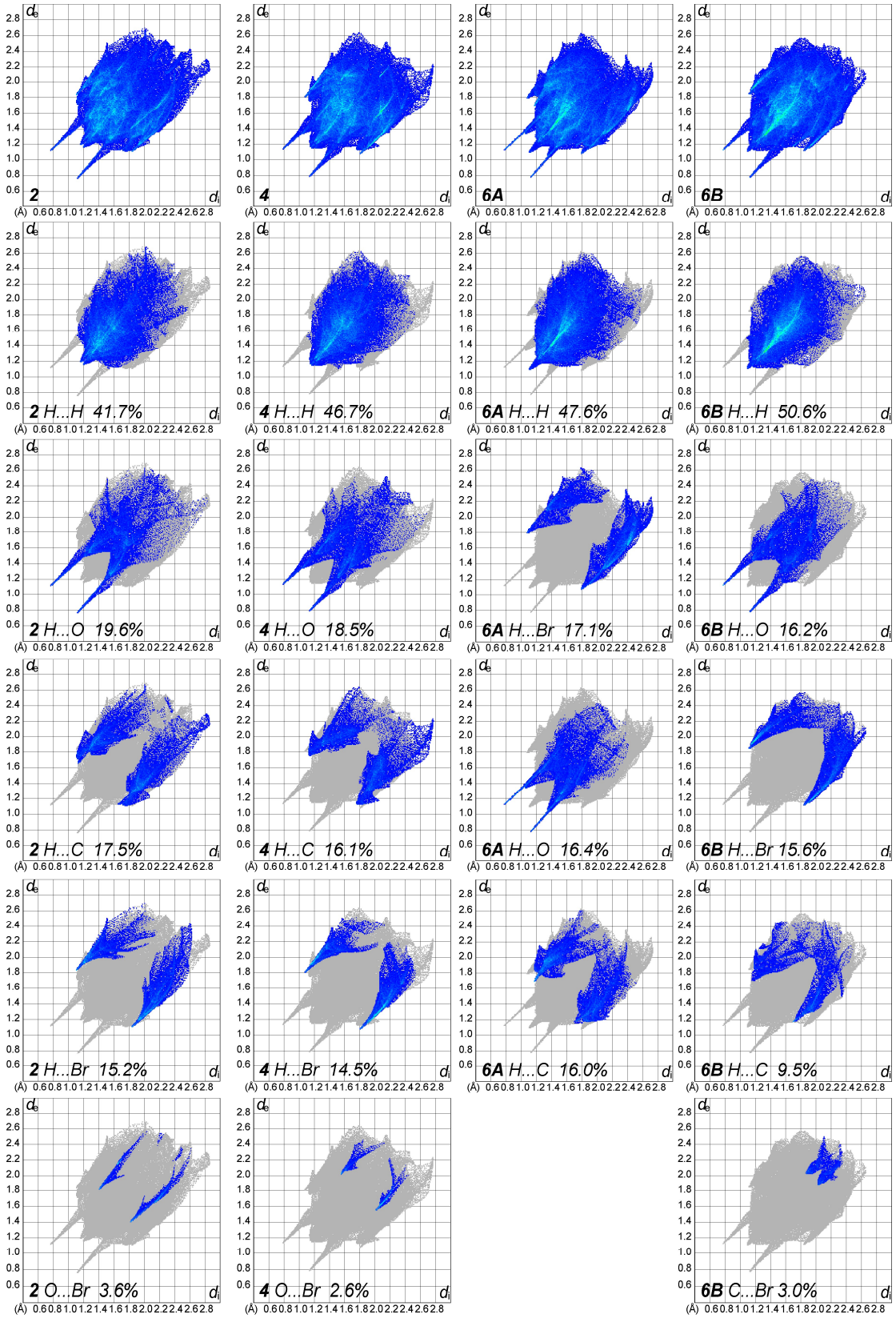

Figure 7 Fingerprint plots for compounds **2**, **4** and **6**, decomposed into contributions from specific intermolecular atom–atom contacts. For each plot, the grey shadow is an outline of the complete fingerprint plot.

View Article Online
DOI: 10.1039/C6CE02210C

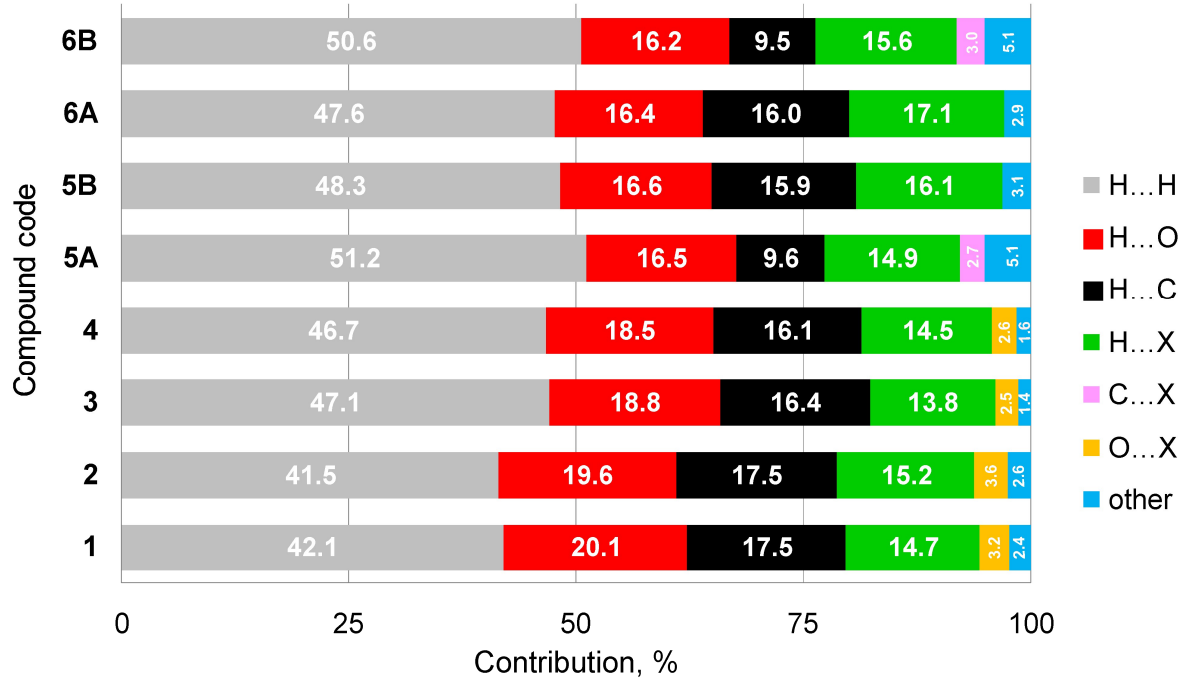

Figure 8 Relative contribution of intermolecular atom–atom contacts to the Hirshfeld surface area.

molecular pairs containing interactions with halogens (–19 to –15 kJ mol^{-1}). According to Hirshfeld analysis, the close contacts are dominated by those associated with relatively weak interactions. Considering diverse pharmaceutical applications of hydantoin derivatives, our investigation of the role of intermolecular interactions involving halogens allows them to be incorporated into strategies for designing new biologically active compounds as well as bio-inspired materials.

Experimental

Cycloalkane-5-spirohydantoins were synthesized by the method of Bucherer[31] and further alkylated at position 3 using the corresponding benzyl halide in K_2CO_3/*N*,*N*-dimethylformamide (Scheme 1).[32] The molecular structures and the purities of the synthesized compounds were confirmed by melting points, elemental analysis, FTIR, ^{1}H and ^{13}C NMR spectroscopy (ESI, Figs S5–S16). Elemental analysis was realized using an Elemental Vario EL III microanalyzer. FTIR spectra were recorded on a Bomem MB 100 spectrophotometer. ^{1}H and ^{13}C NMR spectral measurements were performed on a Bruker AC 200 spectrometer at 200 MHz for the ^{1}H NMR and 50 MHz for the ^{13}C NMR spectra.

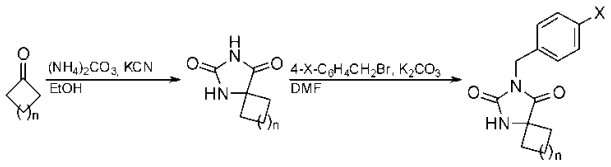

Scheme 1

X-ray structure determinations

Single crystals suitable for an X-ray structure determination were obtained by slow evaporation of acetonitrile solutions at room temperature. Single-crystal X-ray diffraction data were collected on an Oxford Gemini S diffractometer equipped with a sapphire3 CCD detector, using monochromatized Mo $K\alpha$ radiation (λ = 0.71073 Å). Intensities were corrected for absorption by means of analytical (**1**, **4**), multi-scan (**2**, **3**, **5**) and Gaussian (**6**). The structures were solved by direct methods SIR92[33] and refined on F^2 by full-matrix least-squares using the programs SHELXL-97,[34] SHELXL-2014/7[35] and WinGX.[36] All non-hydrogen atoms were refined anisotropically. The positions of H atoms connected to C atoms were calculated on geometric criteria and refined by the riding model with U_{iso} = 1.2U_{eq}(C). Selected crystal data and refinement results for **1**–**6** are listed in Table 7.

CCDC 1509612–1509617 (for **1**–**6**) contain the supplementary crystallographic data for this paper. These data can be obtained free of charge from The Cambridge Crystallographic Data Centre via www.ccdc.cam.ac.uk/data%5Frequest/cif.

Computational Methods

A detailed crystal packing analysis on the title compounds was performed by the PIXELC module[19] from CLP computer program package (version 12.5.2014). Coulombic energies calculated by PIXEL are as accurate as those obtained by rigorous evaluation by quantum mechanics, while the method allows a consistent and reliable parametric estimation of dispersion and repulsion contributions to interaction energies. The lattice energies of the compounds were calculated and the total energy is partitioned into their coulombic, polarization, dispersion and repulsion contributions. Molecular structures for PIXEL analysis are extracted from the X-ray structures, with

View Article Online
DOI: 10.1039/C6CE02210C

Journal Name

ARTICLE

Table 7 Crystallographic and refinement data

Data	1	2	3	4	5	6
Formula	$C_{14}H_{15}ClN_2O_2$	$C_{14}H_{15}BrN_2O_2$	$C_{15}H_{17}ClN_2O_2$	$C_{15}H_{17}BrN_2O_2$	$C_{16}H_{19}ClN_2O_2$	$C_{16}H_{19}BrN_2O_2$
Molecular weight/g mol^{-1}	278.73	323.19	292.76	337.21	306.78	351.23
Crystal system	Monoclinic	Monoclinic	Monoclinic	Monoclinic	Triclinic	Triclinic
Space group	$P\,2_1/n$	$P\,2_1/n$	$P\,2_1/n$	$P\,2_1/n$	$P\bar{1}$	$P\bar{1}$
T/K	298(2)	294(2)	295(2)	295(2)	294(2)	298(2)
a/Å	13.453(3)	13.622(3)	13.287(3)	13.505(3)	6.4340(13)	6.4576(13)
b/Å	5.8751(12)	5.9260(12)	5.9132(12)	5.9344(12)	13.594(3)	13.713(3)
c/Å	17.417(4)	17.379(4)	18.536(4)	18.587(4)	18.649(4)	18.624(4)
α/°	90	90	90	90	72.12(3)	72.03(3)
β/°	101.50(3)	101.00(3)	99.09(3)	97.49(3)	84.92(3)	84.97(3)
γ/°	90	90	90	90	84.41(3)	84.93(3)
V/Å^3	1348.9(5)	1377.1(5)	1438.1(5)	1476.9(5)	1542.0(5)	1559.5(6)
Z	4	4	4	4	4	4
D_c/g cm^{-3}	1.372	1.559	1.352	1.517	1.321	1.496
μ/mm^{-1}	0.282	2.984	0.269	2.790	0.254	2.642
F(000)	584	656	616	688	648	720
Crystal size/mm	0.84×0.14×0.07	0.50×0.14×0.10	0.78×0.20×0.12	0.90×0.26×0.07	0.86×0.12×0.08	0.66×0.14×0.10
θ range/°	3.51–26.73	3.05–26.02	3.45–26.37	3.52–26.37	3.02–26.02	2.99–25.35
Limiting indices	$-17 \le h \le 17$ $-7 \le k \le 7$ $-22 \le l \le 21$	$-14 \le h \le 16$ $-7 \le k \le 7$ $-18 \le l \le 21$	$-16 \le h \le 16$ $-7 \le k \le 7$ $-23 \le l \le 23$	$-16 \le h \le 16$ $-7 \le k \le 7$ $-23 \le l \le 23$	$-7 \le h \le 7$ $-16 \le k \le 16$ $-23 \le l \le 23$	$-7 \le h \le 7$ $-13 \le k \le 16$ $-22 \le l \le 22$
Measured reflections	11741	6989	15320	15743	16450	11272
Independent reflections	2861	2715	2941	3025	6044	5709
Reflections with $I > 2\sigma(I)$	2507	2152	2461	2557	4542	4135
R_{int}	0.0245	0.0240	0.0281	0.0800	0.0233	0.0238
Final R indices [$I > 2\sigma(I)$]	$R_1 = 0.0569$ $wR_2 = 0.1231$	$R_1 = 0.0389$ $wR_2 = 0.0833$	$R_1 = 0.0477$ $wR_2 = 0.1109$	$R_1 = 0.0686$ $wR_2 = 0.1540$	$R_1 = 0.0566$ $wR_2 = 0.1236$	$R_1 = 0.0452$ $wR_2 = 0.1222$
R indices (all data)	$R_1 = 0.0657$ $wR_2 = 0.1279$	$R_1 = 0.0553$ $wR_2 = 0.0901$	$R_1 = 0.0597$ $wR_2 = 0.1173$	$R_1 = 0.0768$ $wR_2 = 0.1630$	$R_1 = 0.0807$ $wR_2 = 0.1355$	$R_1 = 0.0690$ $wR_2 = 0.1357$
S	1.107	1.023	1.071	1.174	1.049	1.068
Parameters	172	172	181	182	379	379
$\Delta\rho_{max}$, $\Delta\rho_{min}$/e Å^{-3}	0.264, –0.311	0.475, –0.493	0.220, –0.363	0.635, –1.634	0.366, –0.256	0.528, –0.586

hydrogen atoms relocated to their usual values (C–H distance 1.08 Å, O–H and N–H distance 1.00 Å). The molecular electron densities for the PIXEL energy calculations were derived at the MP2/6-31G(d,p) level using Gaussian 09 program package.[37] Hirshfeld surfaces[18] and the associated 2D-fingerprint plots[18b] were generated using CrystalExplorer 3.1.[38] Hirshfeld surfaces mapped with different properties e.g. d_e, d_{norm}, shape index, curvedness, have proven to be a useful visualization tool for the analysis of intermolecular interactions and the crystal packing behavior of molecules.[18] The d_i and d_e are functions of distances from the Hirshfeld surface to the nearest nucleus inside the surface and outside the surface, respectively, while the d_{norm} combines both d_e and d_i, each normalised by the van der Waals radius for the particular atoms involved in the close contact to the surface.[18] The 2D fingerprint plots were constructed using d_i and d_e in the translated 0.4–3.0 Å range. The 2D fingerprint plot provides decomposition of Hirshfeld surfaces into contribution of different intermolecular interactions in the crystal structure. Therefore, both Hirshfeld surfaces and fingerprint plots enable the comparison of intermolecular interactions which build different supramolecular structures.

Acknowledgements

This work was supported by the Ministry of Education, Science and Technological Development of the Republic of Serbia (Projects no. 172013, 172035 and III45007).

Notes and references

1 C. R. Groom and F. H. Allen, *Angew. Chem. Int. Ed.* 2014, **53**, 662.
2 A. J. Cruz-Cabeza and C. H. Schwalbe, *New. J. Chem.*, 2012, **36**, 1347.

View Article Online
DOI: 10.1039/C6CE02210C

3 B. LeDuc, Antiseisure agent, In: Foye's principles of medicinal chemistry, 6th ed., T. Lemke and D. Williams, Eds. Philadelphia, PA: Lippincott Williams & Wilkins, 2008.
4 A. S. Troupin, P. Friel, M. P. Lovely and A.J. Wilensky, *Ann. Neurol.*, 1979, **6**, 410.
5 W. D. Hooperer, N. J. Oshea and M. S. Qing, *Chirality*, 1992, **4**, 142.
6 (a) J. Handzlik, M. Bajda, M. Zygmunt, D. Maciąg, M. Dybała, M. Bednarski, B. Filipek, B. Malawska and K. Kieć-Kononowicz, Bioorg. Med. Chem., 2012, 20, 2290; (b) N. Singh, J. N. Sinha, S. K. Rastogi, P. R. Dua and R. P. Kohli, Japan J. Pharmacol., 1971, 21, 755; (c) D. Bracchetti, F., Naccarella, M. Palmieri, M. Fulvi and P. C. Pavesi, *J. Cardiovasc. Pharm.*, 1989, **14**, S79.
7 (a) F. Fujisaki, K. Toyofuku, M. Egami, S. Ishida, N. Nakamoto, N. Kashige, F. Miake and K. Sumoto, *Chem. Pharm. Bull.*, 2013, **61**, 1090; (b) J. Handzlika, E. Szymańska, S. Alibert, J. Chevalier, E. Otrębska, E. Pękala, J.-M. Pagès and K. Kieć-Kononowicz, *Bioorg. Med. Chem.*, 2013, **21**, 135.
8 (a) G. Spengler, M. Evaristo, J. Handzlik, J. Serly, J. Molnár, M. Viveiros, K. Kieć-Kononowicz and L. Amaral, *Anticancer Res.*, 2010, **30**, 4867; (b) H. A. Mohamed, N. M. R. Girgis, R. Wilcken, M. R. Bauer, H. N. Tinsley, B. D. Gary, G. A. Piazza, F. M. Boeckler and A. H. Abadi, *J. Med. Chem.*, 2011, **54**, 495; (c) M. Mudit, F. A. Behery, V. B. Wali, P. W.Sylvester and K. A. El Sayed, *Nat.Prod. Comm.*, 2010, **5**, 1623.
9 (a) A. Camerman and N. Camerman, *Science*, 1970, **168**, 1457; (b) G. P. Jones and P. R. Andrews, *J. Chem. Soc. Perkin Trans. II*, 1987, 415; (c) M. L. Brown, G. B. Brown and W. J. Brouillette, *J. Med. Chem.*, 1997, **40**, 602.
10 G. M. Lipkind and H. A. Fozzard, *Mol. Pharmacol*., 2010, **78**, 631.
11 G. R. Desiraju, *Chem. Comm.*, 1997, 1475.
12 A. Gavezzotti and L. L. Presti, *Cryst. Growth Des.*, 2016, **16**, 2952.
13 G. R. Desiraju, *Acc. Chem. Res.*, 2002, **35**, 565.
14 A. Kovács and Z. Varga, *Coordin. Chem Rev.*, 2006, 250, 710.
15 (a) P. Politzer, J. S. Murray and T. Clark, *Phys. Chem. Chem. Phys.*, 2010, **12**, 7748; (b) X. Ding, M. Tuikka and M. Haukka; Halogen Bonding in Crystal Engineering in J. B. Benedict (ed.) Recent Advances in Crystallography, 2012, In Tech, New York, 143.
16 K. E. Riley and P. Hobza, *Phys. Chem. Chem. Phys.*, 2013, **15**, 17742.
17 P. –P. Zhou, W. –Y. Qiu, S. Liub and N. –Z. Jin, *Phys. Chem. Chem. Phys*., 2011, **13**, 7408.
18 (a) M. A. Spackman and D. Jayatilaka, *CrystEngComm*, 2009, **11**, 19; (b) M.A. Spackman, J.J. McKinnon, *CrystEngComm*, 2002, **4**,378; (c) J.J. McKinnon, M.A. Spackman and A.S. Mitchell, *Acta Cryst.*, 2004, **60B**, 627; (d) S. K. Seth, D. Sarkar and T. Kar, *CrystEngComm*, 2011, **13**, 4528; (e) D. A. Safin, K. Robeyns and Y. Garcia, *CrystEngComm*, 2016, **18**, 7284.
19 (a) A. Gavezzotti, Molecular Aggregation, Oxford University Press, Oxford, 2005, ch. 12; (b) A. Gavezzotti, *J. Phys. Chem. B*, 2003, **107**, 2344; (c) A. Gavezzotti, *Mol. Phys.*, 2008, **106**, 1473.
20 (a) B. Chattopadhyay, A. K. Mukherjee, N. Narendra, H. P. Hemantha, V. V. Sureshbabu, M. Helliwell and M. Mukhherjee, *Cryst. Growth Des.*, 2010, **10**, 4476; (b) S. Graus, S. Uriel and J. L. Serrano, *Cryst. Eng. Comm.*, 2012, **14**, 3759; (c) S. Graus, D. Casabona, S. Uriel, C, Cativiela and J. L. Serrano, *Cryst. Eng. Comm.*, 2010, **12**, 3132; (d) P. T. Todorov, R. N. Petrova, E. D. Naydenova and B. L. Shivachev, *Cent. Eur. J. Chem.*, 2009, **7**, 14.
21 S. Hmuda, N. Trišović, J. Rogan, D. Poleti, Ž. Vitnik, V. Vitnik, N. Valentić, B. Božić and G. Ušćumlić, *Monats. Chem.*, 2014, **145**, 821.
22 (a) I. Dance, *New J. Chem.*, 2003, **1**, 22; (b) D. Dey, C. S. Shripanavar, K. Banerjee and D. Chopra, *J. Crystalograph.*, 2014, doi: 10.1155/2014/585282.
23 Y. Gu, T. Kar and S. Scheiner, *J. Am. Chem. Soc.*, 1999, **121**, 9411.
24 (*a*) H. Masu, Y. Sagara, F. Imabeppu, H. Takayanagi, K. Katagiri, M. Kawahata, M. Tominaga, H. Kagechika, K. Yamaguchia and I. Azumaya, *CrystEngComm*, 2011, **13**, 406; (*b*) A. J. Cruz Cabeza, G. M. Day, W. D. S. Motherwell and W. Jones, *Cryst. Growth Des.*, 2006, **6**, 1858; (c) F. H. Allen, C. M. Bird, R. S. Rowland, S. E. Harris and C. H. Schwalbe, *Acta Cryst.*, 1995, **B51**, 1068.
25 C. Ouvrard, J.-Y. Le Questel, M. Berthelot and C. Laurence, *Acta Cryst.*, 2003, **59B**, 512.
26 (a) A. R. Voth, P. Khuu, K. Oishi and P. S. Ho, *Nat. Chem.*, 2009, **1**, 74; (b) M. R. Scholfield, C. M. Vander Zanden, M. Carter and P. S. Ho, *Protein Sci.*, 2013, **22**, 139.
27 H. Matter, M. Nazar, S. Güssregen, D. W. Will, H. Schreuder, A. Bauer, M. Urmann, K. Ritter, M. Wagner, and V. Wehner, *Angew. Chem. Int. Ed.*, 2009, **48**, 2911.
28 A. J. Rybarczyk-Pirek, L. Checinska, M. Malecka and S. Wojtulewski, *Cryst. Growth Des.*, 2013, **13**, 3913.
29 A. J. Rybarczyk-Pirek, M. Łukomska-Rogala, S. Wojtulewski and M. Palusiak, *Cryst. Growth Des.*, 2015, **15**, 5802.
30 Y. –H. Luo and B. –W. Sun, *CrystEngComm*, 2013,15, 7490
31 H. T. Bucherer and V. A. Lieb, *J. Prakt. Chem.*, 1934, **141**, 5.
32 H. Suzuki, M. B. Kneller, D. A. Rock, J. P. Jones, W. F. Trager and A. E. Rettie, *Arch. Biochem. Biophys.*, 2004, **429**, 1.
33 A. Altomare, G. Cascarano, C. Giacovazzo, A. Guagliardi, M. C. Burla, G. Polidori and M. Camalli, *J. Appl. Crystallogr.*, 1994, **27**, 435.
34 G. M. Sheldrick, *Acta Crystallogr.*, 2008, **A64**, 112.
35 G. M. Sheldrick, *Acta Crystallogr.*, 2015, **C71**, 3.
36 L. J. Farrugia, *J. Appl. Crystallogr.*, 2012, **45**, 849.
37 M. J. Frisch, G. W. Trucks, H. B. Schlegel, G. E. Scuseria, M. A. Robb, J. R. Cheeseman, G. Scalmani, V. Barone, B. Mennucci, G. A. Petersson, H. Nakatsuji, M. Caricato, X. Li, H. P. Hratchian, A. F. Izmaylov, J. Bloino, G. Zheng, J. L. Sonnenberg, M. Hada, M. Ehara, K. Toyota, R. Fukuda, J. Hasegawa, M. Ishida, T. Nakajima, Y. Honda, O. Kitao, H. Nakai, T. Vreven, J. A. Montgomery Jr, J. E. Peralta, F. Ogliaro, M. Bearpark, J. J. Heyd, E. Brothers, K. N. Kudin, V .N. Staroverov, R. Kobayashi, J. Normand, K. Raghavachari, A. Rendell, J. C. Burant, S. S. Iyengar, J. Tomasi, M. Cossi, N. Rega, J. M. Millam, M. Klene, J. E. Knox, J. B. Cross, V. Bakken, C. Adamo, J. Jaramillo, R. Gomperts, R. E. Stratmann, O. Yazyev, A. J. Austin, R. Cammi, C. Pomelli, J. W. Ochterski, R. L. Martin, K. Morokuma, V. G. Zakrzewski, G. A. Voth, P. Salvador, J. J. Dannenberg, S. Dapprich, A. D. Daniels, Ö. Farkas, J. B. Foresman, J. V. Ortiz, J. Cioslowski and D. J. Fox, Gaussian 09, Revision D.01. Wallingford CT: Gaussian Inc., 2009.
38 S. K. Wolff, D. J. Grimwood, J. J. McKinnon, M. J. Turner, D. Jayatilaka and M. A. Spackman, CrystalExplorer (Version 3.1), University of Western Australia, 2012.

View Article Online
DOI: 10.1039/C6CE02210C

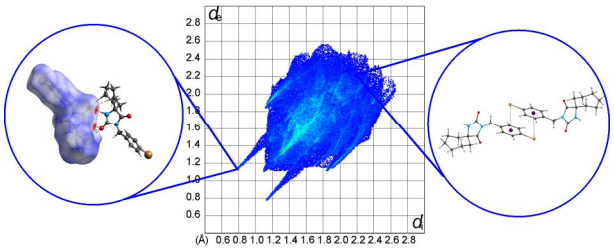

A detailed crystal structure analysis of a series of cycloalkanespiro-5-hydantoins bearing a halogeno substituted benzyl moiety has been performed by Hirshfeld surface analysis and the PIXEL method with the emphasis on the intermolecular interactions involving halogens.